Planetary Nebulae: An Eye to the Future
Proceedings IAU Symposium No. 283, 2011
A. Manchado, L. Stanghellini & D. Schönberner, eds.

doi:10.1017/S1743921312011064

PNe in NGC 300: Their abundances and chemical gradients†

Miiriam Peña[1], Grazyna Stasinska[2], Fabio Bresolin[3] and Yiannis Tsamis[4]

[1]Instituto de Astronomia, UNAM. Apdo. Postal 70264, 04510 Mexico D.F.,
email: miriam@astro.unam.mx

[2]LUTH, Observatoire de Paris,5 Place Jules Janssen 92190 Meudon, France
email: grazyna.stasinska@obspm.fr

[3]Institute for Astronomy, 2680 Woodlan Drive, Honolulu, Hi 96822, USA
email: bresolin@ifa.hawaii.edu

[4]ESO, Karl-Schwarzchild Str. 2, D-85748 Garching bei Munchen, Germany
email: ytsamis@eso.org

Abstract. Spectrophotometric data of a number of planetary nebulae and compact HII regions of NGC 300 have been obtained with the FORS 2 spectrograph of the VLT. We present a preliminary analysis of such data.

Keywords. Galaxies: individual (NGC 300), planetary nebulae: general, ISM: abundances

1. Introduction

Extragalactic planetary nebulae (PNe) are most valuable objects to analyze the chemical composition of the ISM at the time of formation of their central stars and the stellar evolution of low-intermediate mass stars (LIMS). Interesting problems such as how LIMS enrich the ISM, or the presence of inhomogeneities and chemical gradients in galaxies, the galactic kinematics and the distances to external galaxies through the PNe luminosity function (PNLF), can be studied with PNe.

So far, with our group, we have analyzed the PNe in two dwarf irregular galaxies: NGC 3109 (Peña *et al.* 2007) and NGC 6822 (Hernández-Martínez *et al.* 2009). Now we are studying the PN population in NGC 300, a nearby spiral galaxy in the Sculptor Group, at a distance of 1.88 Mpc (Gieren *et al.* 2006).

Several studies have been performed in NGC 300, relative to its massive stars, HII regions, etc. Bresolin *et al.* (2009) carried out a deep analysis of the giant HII regions at different galactocentric distances in this galaxy, deriving their chemical abundances. These authors reported an abundance gradient of -0.077 dex/kpc, with a central metallicity of $12+\log \mathrm{O/H} \sim 8.57$.

2. Our work

2.1. *Direct imaging*

In 2006 we started an observational program aiming to find a large number of PNe in NGC 300 and to analyze their chemical behavior. The Very Large Telescope (VLT-ESO) equipped with the FORS 2 spectrograph was used for this purpose. [OIII] 5007 on-band off-band pre-imaging, with the filters FILT-500-5 and OIII/6000, was obtained to search

† Based on observations collected at the ESO-VLT Observatory, Paranal, Chile, program ID077.B-04330.

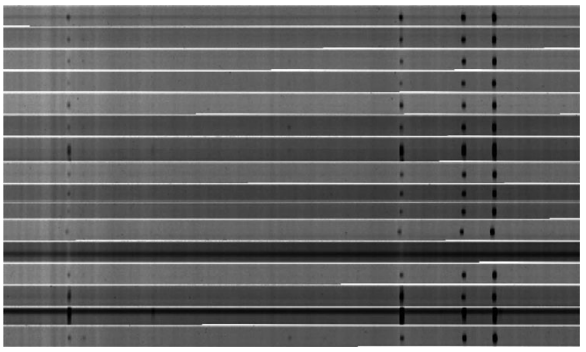

Figure 1. Blue spectra, covering from Hγ to [OIII]5007 Å, of some emission line objects of the central zone of NGC 300. Some compact HII regions and PNe are clearly detected.

for emission line objects in two zones of the galaxy. FORS 2 has a field of view of 6.8× 6.8 arcmin and we covered a central zone (centered at R.A. 00:54:49.0, Dec −37:41:02.0) which includes the central region of the galaxy and an outskirts zone (centered at R.A. 00:55:22.0, Dec −37:43:00.0).

After subtracting the on-band − off-band images, we searched for emission line objects in both zones. Hundreds of such objects were found. PN candidates were selected as those stellar objects with no central star detected in the off-band image. More than a hundred PN candidates were detected in both galactic zones: about 68 in the central zone and more than 30 in the external one. We rediscovered most of the 34 PN candidates reported by Soffner *et al.* (1996). Some of Soffner *et al.*'s objects were reclassified as compact HII regions and some of them were not confirmed as emission line objects. A deep analysis with the results from our pre-imaging data will be published elsewhere (Peña *et al.* 2011, in preparation).

We selected a number of PN candidates and other emission line objects for follow-up spectroscopy with FORS 2 in MXU mode.

2.2. *Spectroscopy*

Multiobject FORS2-MXU spectra of around 50 emission line objects, chosen from the on-band off-band pre-imaging, were obtained on August 2006. Three grisms were used to cover the widest wavelength range possible: 600B (3600-5100 Å), 600RI (5000-7500 Å), and 300I (6500-9500 Å). Total exposure times were between 5 and 3.3 hr for observations with grism 600B, between 3.8 and 1.9 hr for observations with grism 600RI, and between 2 and 0.5 hr, for observations with grism 300I. Three standard stars were observed each night for flux calibration. Bidimensional frames containing the spectral data were reduced with the standard procedures by using the EsoRex pipeline provided by the ESO: bias subtraction, flat fielding, and wavelength calibrations were applied. Afterwards we used standard IRAF† tasks for spectral extraction and flux calibration.

In Fig. 1 some spectra in the blue wavelength range (grism 600B), for objects in the central zone, are shown. These spectra have been already reduced (bias subtracted, flat fielded and calibrated in wavelength).

† IRAF is distributed by the NOAO, which is operated by the AURA, Inc., under cooperative agreement with the NSF.

https://doi.org/10.1017/S1743921312011064 Published online by Cambridge University Press

3. Results

As already said, the spectra for each observed object were extracted from the 2D frames (Fig. 1) and calibrated in flux. Then all the available lines were measured. Electron temperatures and densities were derived from several diagnostic lines. We selected those objects where the temperature sensitive [OIII] 4363/5007 line ratio and the density sensitive [SII] 6717/6730 line ratio were measured with S/N better than 3, in order to derive ionic abundances. Total abundances were then obtained from the ionic abundances and by employing the ionization correction factors (icf's) by Kingsburgh & Barlow (1994). In total we determined abundances for 18 PNe and 9 compact HII regions.

3.1. *Physical conditions of PNe in comparison to HII regions*

We have compared the physical conditions of our PN sample with those of our compact HII region candidates and of the giant HII regions from Bresolin *et al.* (2009). We found that:

a.– PNe and HII regions cover a similar O/H abundance ratio range, from 8. $1 < 12 + \log \mathrm{O/H} < 8.6$.

b.– PNe show higher ionization degree than HII regions, due to their hotter central stars.

c.– They also show higher electron temperatures and larger densities.

d.– And, according to their much fainter central stars, PNe present lower Hβ luminosities than HII regions.

All the above properties of PNe in relation to those in HII regions, confirm that our PN sample actually consist of bona-fide PN candidates.

3.2. *Chemical abundance behavior*

Chemical abundances derived for PNe were compared to those derived for HII regions. We found that PNe show:

1.– much higher N/O, which is expected because it is known that PN progenitors produce N and C and contaminate their surfaces with these products. Among our PN sample, three Peimbert Type I PNe were found, which represents 17% of the analyzed sample. This proportion is similar to the one found in the Milky Way.

2.– Interestingly, in average PNe show higher Ne/O abundance ratio than HII regions by about 0.1 dex. This apparent Ne overabundance has been reported for several PNe samples, when compared to HII regions and Blue Compact Galaxies (see, e.g., Milingo *et al.* 2010). It has been interpreted as an extra amount of Ne produced by PN central stars. We consider that this corresponds more to a problem with the icf's used for Ne, because when we plot the Ne/O ratio as a function of the ionization degree as given by $\mathrm{O^{++}}/\ (\mathrm{O^{++}}+\mathrm{O^{+}})$, for PNe and HII regions in NGC 300, a clear dependence is found: Ne/O increases with the ionization degree. Log Ne/O is about -1.1 for low ionization objects and increases up to a maximum (-0.7) for objects with $\mathrm{O^{++}}/\ (\mathrm{O^{++}}+\mathrm{O^{+}}) > 0.7$. A similar behavior was found by Peimbert *et al.* (1992) when analyzing the Ne/O ratio in different zones of the galactic HII region M17: low-ionization zones show lower Ne/O ratios.

3.– In addition, PNe present lower S/O abundance ratios than HII regions, by about 0.3 dex. This result has been reported previously for other PN samples and it has been called the "S anomaly" (Henry *et al.* 2004; Kwitter 2011, this volume). It has been attributed to inadequate icf's for S determination which do not take into account properly the presence of $\mathrm{S^{+3}}$ in PNe.

4.– On the other hand, Ar/O abundance ratios in our PNe are similar to the ones found for HII regions, suggesting that icf's for Ar are adequate.

https://doi.org/10.1017/S1743921312011064 Published online by Cambridge University Press

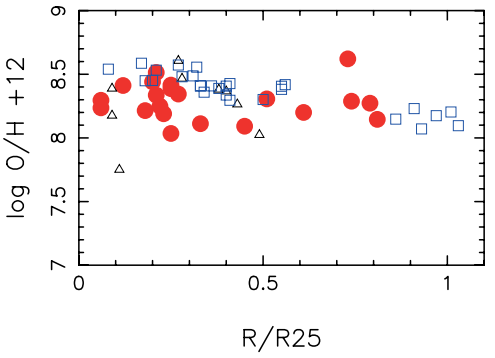

Figure 2. The O abundance gradient for PNe (red dots) and giant HII regions (blue squares). Black triangles represent compact HII regions. The gradient for PNe is much flatter than for HII regions, mostly due to the lower O abundance of central PNe.

3.3. *The abundance gradients in NC 300*

The behavior of O, Ne and Ar abundances of PNe as function of the distance to the galactic center of NGC 300 were analyzed and compared to the abundance gradients derived for HII regions. As said in the introduction, HII regions present an O abundance gradient of −0.77 dex per kpc. We determined the de-projected distance of each of our PNe to the galactic center in the same way as Bresolin *et al.* (2009) did for HII regions, and derived the O galactic gradient provided by PNe. The behavior of log O/H + 12 vs. the galactocentric distance (in units of R_{25}) for PNe and HII regions, is presented in Fig. 2. One can see that the PN oxygen abundances show a larger dispersion than HII region oxygen abundances and a smaller gradient. This smaller gradient is mainly due to the low O abundances for the PNe in the central zone of the galaxy. This could be explained if central PNe belong to a much older population. Other effects, such as the ON cycle occurring in many central PNe and lowering their O abundances, or migration of old PNe towards different galactic orbits can modify the gradient, making it flatter. We are analyzing other element abundance gradients. An extensive discussion will be presented in the near future (Peña *et al.* 2012, in preparation).

Acknowledgements

This work received partial support from DGAPA-UNAM grant IN105511.

References

Bresolin, F., Gieren, W., Kudritzk, R.-P., *et al.* 2009, *ApJ*, 700, 309
Gieren, W., Pietrzyński, G., Nalewajko, K., *et al.* 2006, *ApJ*, 647, 1056
Henry, R., Kwitter, K., & Balick, B. 2004, *AJ*, 127, 2284
Hernández-Martínez, L., Peña, M., Carigi, L., & García-Rojas, J. 2009, *A&A*, 505, 1027
Kingsburgh, R. & Barlow, M. J. 1994, *MNRAS*, 271, 257
Kwitter, K 2011, in: A. Manchado, L. Stanghellini & D. Schönberner (eds.), *Planetary Nebulae: An Eye to the Future*, IAU Symp. 283, this volume
Milingo, J. B., Kwitter, K. B., Henry, R. B. C., & Souza, S. P. 2010, *ApJ*, 711, 619
Peimbert, M., Torres-Peimbert, S., & Ruiz, M. T. 1992, *Rev Mexicana AyA*, 24, 155
Peña, M., Stasiǹska, G., & Richer, M. 2007, *A&A*, 476, 745
Soffner, T., Méndez, R., Jacoby, G. H., *et al.* 1996, *A&A*, 306, 9

https://doi.org/10.1017/S1743921312011064 Published online by Cambridge University Press